VILNIUS UNIVERSITY
FACULTY OF CHEMISTRY AND GEOSCIENCES
INSTITUTE OF CHEMISTRY
DEPARTMENT OF ORGANIC CHEMISTRY

Markas Kasparavichius
Pharmaceutical Chemistry
Master's Thesis

9, 10-DIALKYNYLANTHRACENE EMITTERS FOR LIGHT UPCONVERSION APPLICATIONS

Scientific advisor
Prof. Dr. Edvinas Orentas

Vilnius 2026

TABLE OF CONTENTS

LIST OF ABBREVIATIONS 3
INTRODUCTION 5
I. LITERATURE REVIEW 7
I.1. TTA-UC Mechanism and Quantum Yield Parameters 7
I.2. High-Performance Annihilators 8
I.3. Anthracene Derivatives in TTA-UC 10
I.4. Synthetic Methods for 9,10-Diethynylanthracenes 11
I.5. Applications of TTA-UC 12
II. RESULTS AND DISCUSSION 15
II.1. Sonogashira Coupling 16
II.2. Lithium Acetylide Synthesis and Nucleophilic Substitution 18
II.3. Synthesis of Tin-Containing Anthracene Derivatives 19
II.4. Synthesis of the Adamantyl Derivative 20
II.5. Photophysical Properties and Upconversion Performance 20
III. EXPERIMENTAL PART 25
III.1. Instrumentation 25
III.2. Materials 25
CONCLUSIONS 32
SUMMARY 33
REFERENCES 34

LIST OF ABBREVIATIONS

Ad – adamantyl
AcOH – acetic acid
Ar – aryl
aq. – aqueous
BPEA – 9,10-bis(phenylethynyl)anthracene
bTB – 9,10-bis(alkyl)-bridged anthracene (two-bridge scaffold, TB = two bridges)
Bu – butyl
DB – doubly bridged (anthracene scaffold)
DPA – 9,10-diphenylanthracene
DPND – dipyrrolonaphthyridinedione
DPP – diketopyrrolopyrrole
DSSC – dye-sensitized solar cell
EQE – external quantum efficiency
Et – ethyl
Et_2O – diethyl ether
Et_3N – triethylamine
EtOAc – ethyl acetate
f – spin-statistical factor (probability of singlet formation in TTA)
FL – fluorescence
HMPA – hexamethylphosphoramide
HL-RISC – high-level reverse intersystem crossing
iPr – isopropyl
ISC – intersystem crossing
LDA – lithium diisopropylamide
Me – methyl
MeOH – methanol
M.p. – melting point
MW – microwave
NBS – *N*-bromosuccinimide
NIR – near-infrared
NMR – nuclear magnetic resonance
OLED – organic light-emitting diode
PdOEP – palladium(II) octaethylporphyrin
PdTPBP – palladium(II) tetraphenylbenzoporphyrin
PDT – photodynamic therapy
PLGA – poly(lactic-co-glycolic acid)
PPh_3 – triphenylphosphine
PtOEP – platinum(II) octaethylporphyrin
r.t. – room temperature
SF – singlet fission
TBAF – tetrabutylammonium fluoride
TES – triethylsilyl
TET – triplet energy transfer
THF – tetrahydrofuran
TIPS – triisopropylsilyl
TIPSA – triisopropylsilyl acetylene
TIPS-Ac – 9,10-bis((triisopropylsilyl)ethynyl)anthracene
TLC – thin-layer chromatography
TMS – trimethylsilyl

TMSA – trimethylsilyl acetylene
TPhC – triphenylmethyl (trityl)
TPhS – triphenylsilyl
T_1 – first excited triplet state
T_2 – second excited triplet state
TTA – triplet-triplet annihilation
TTA-UC – triplet-triplet annihilation upconversion
UC – upconversion
φ^{FL} – fluorescence quantum yield
φ^{ISC} – intersystem crossing quantum yield
φ^{TET} – triplet energy transfer quantum yield
φ^{TTA} – triplet-triplet annihilation quantum yield
φ^{UC} – upconversion quantum yield
vis-visible (light/spectrum)

INTRODUCTION

Triplet-triplet annihilation upconversion (TTA-UC) is a photophysical process in which two low-energy photons are converted into one photon of higher energy through sensitized triplet excitation followed by bimolecular annihilation [1,2]. Because it operates under low-intensity, non-coherent illumination – including sunlight – TTA-UC is actively pursued for applications in solar energy harvesting, photocatalysis, biological imaging, and photodynamic therapy [3,4].

9,10-Disubstituted anthracenes are among the most studied and practically important annihilator classes for TTA-UC. Several of their properties make them well suited to address the needs of these application areas. Their triplet energy levels ($T_1 \approx 1.7–1.8$ eV) match the output of widely available and efficient porphyrin sensitizers, enabling efficient Dexter-type triplet energy transfer [5,6]. High fluorescence quantum yields – φ_{FL} approaching unity for 9,10-diphenylanthracene (DPA) [5] – translate directly into high upconversion quantum yields, which is critical for solar and photocatalytic applications where photon flux is limited. The emission of anthracene derivatives in the blue-to-green spectral region (420–510 nm) overlaps with the absorption of many biological chromophores and photosensitizers, making them relevant for bioimaging and photodynamic therapy [7,8]. Finally, the well-established reactivity of the 9,10-positions allows systematic structural variation, which is essential for tuning the TTA efficiency φ_{TTA} and the spin-statistical factor *f* that determine how efficiently triplet pairs are converted into emissive singlets [9,10].

The introduction of alkynyl substituents at the 9,10-positions – in particular silylethynyl groups – extends the capabilities of the anthracene scaffold further. Bulky silyl groups attached *via* an alkyne linker prevent the photodimerization and π-aggregation that quench fluorescence at the concentrations required for efficient TTA [6,11]. The alkyne linker simultaneously extends conjugation, enabling spectral tuning and large anti-Stokes shifts: 9,10-bis((triisopropylsilyl)ethynyl)anthracene (TIPS-Ac) achieves near-infrared-to-blue upconversion that is directly relevant to biological imaging in the tissue transparency window [6]. In TIPS-substituted acenes, the interaction of silicon with the π-system through σ–π* hyperconjugation has been proposed as an additional factor affecting fluorescence efficiency [4,12], though its exact contribution in the 9,10-diethynylanthracene series has not been quantified. Together, these properties make 9,10-diethynylanthracene derivatives a structurally tunable annihilator platform capable of meeting the requirements of multiple TTA-UC application fields simultaneously.

Despite this potential, the structure–property relationships within the 9,10-diethynylanthracene family remain poorly explored. How does changing the group-14 central atom (Si *vs.* Ge) affect fluorescence efficiency and TTA performance? What is the role of substituent bulk independently of electronic effects? How does extending the alkyne spacer modify the annihilator energy levels? Answering these questions requires a systematically designed compound library evaluated under identical conditions. This work presents the synthesis and photophysical characterization of eight such derivatives, providing a direct comparative dataset and evidence-based design guidelines for expanding the range of efficient anthracene-based TTA-UC annihilators.

The **aim** of this work is to synthesize a series of 9,10-diethynylanthracene derivatives bearing structurally diverse substituents and to establish quantitative structure–property relationships for their performance as TTA-UC annihilators.

Objectives:

1. To synthesize target 9,10-diethynylanthracene derivatives bearing trialkylsilyl, triarylsilyl, triphenylmethyl, and trialkylgermyl substituents.

2. To evaluate and optimize reaction conditions for both synthetic routes and to investigate the influence of reaction parameters (temperature, microwave irradiation, solvent, base) on yield and selectivity.

3. To measure φ_{UC}, φ_{FL}, φ_{TTA}, and f for all synthesized annihilators in THF/PtOEP system and to benchmark them against DPA and TIPS-Ac.

4. To analyze the influence of substituent type (C vs. Si vs. Ge central atom), steric bulk, and alkyne spacer length on the photophysical parameters and to identify the structural features that maximize TTA-UC efficiency.

5. To investigate synthetic approaches toward tin-containing and adamantyl-substituted 9,10-diethynylanthracene derivatives, identify the obstacles encountered, and propose strategies for future work.

I. LITERATURE REVIEW

I.1. TTA-UC Mechanism and Quantum Yield Parameters

Triplet-triplet annihilation upconversion (TTA-UC) is a photophysical process in which two low-energy photons are converted into one photon of higher energy [1–3,13,14]. Modern interest in TTA-UC is driven by its main practical advantage over other types of upconversion - it works at low excitation power densities (around a few mW/cm^2), using non-coherent light sources, which makes it relevant for solar energy, bioimaging and photocatalysis [15,16].

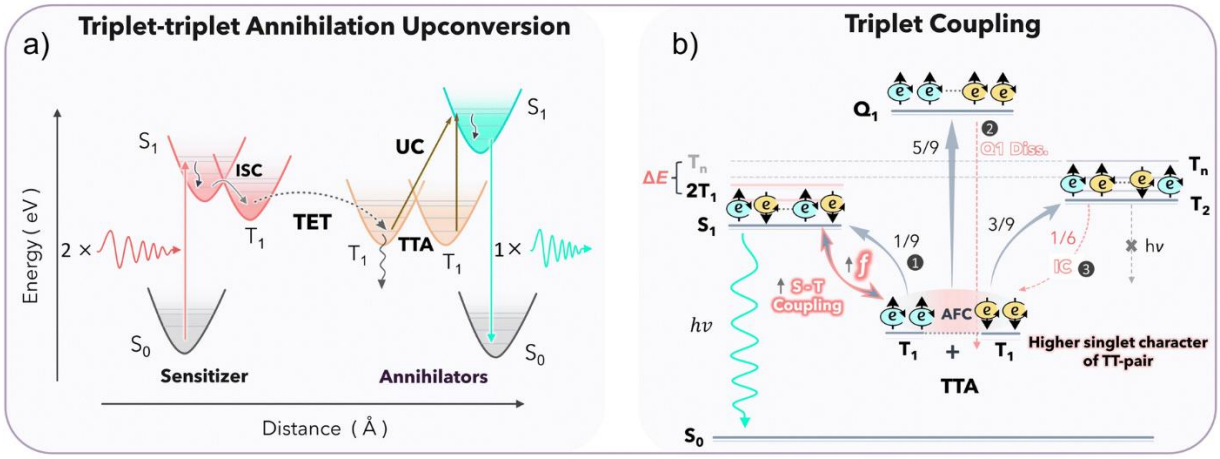

Scheme 1.1. *(a) Scheme of TTA-UC; (b) schematic illustration of the post-TTA events resulting in the formation of the TT pair with singlet (S_1, f = 1/9), triplet (T_2, 3/9) and quintet (Q_1, 5/9) states due to the anti-ferromagnetic coupling (AFC) between triplet-pairs.[13]*

A typical TTA-UC system has two components: a sensitizer and an annihilator (emitter). The sensitizer absorbs low-energy photons and efficiently reaches its excited triplet state *via* intersystem crossing (ISC). It then transfers this energy to an annihilator molecule through a short-range, collision-based Dexter mechanism - a process called triplet energy transfer (TET). When two annihilators in their excited triplet state T_1 collide, they can undergo triplet-triplet annihilation (TTA) to produce one molecule in the high-energy singlet excited state S_1 and one in the ground state S_0. This S1 state then emits a fluorescence photon with shorter wavelength than the original excitation –the upconverted photon [13,15].

The overall upconversion quantum yield φ_{UC} is given by the product of the efficiencies of each step:

$$\varphi_{UC} = ½ \cdot \varphi_{ISC} \cdot \varphi_{TET} \cdot \varphi_{TTA} \cdot \varphi_{FL}$$

where φ_{ISC} is the intersystem crossing quantum yield in the sensitizer, φ_{TET} is the triplet energy transfer efficiency from sensitizer to annihilator, φ_{TTA} is the probability of singlet state formation after TTA, and φ_{FL} is the fluorescence quantum yield of the annihilator. The factor ½ reflects the stoichiometry: at least two low-energy photons are required to generate one high-energy photon, setting the theoretical maximum at φ_{UC} = 50% [1,14,17].

Table 1.1. *Parameters of TTA-UC quantum yield and their main determining factors.*

Parameter	Typical range	Main determining factors
φ_{ISC}	60–100%	Spin-orbit coupling strength; heavy-atom effect (e.g. Pt, Pd); sensitizer structure
φ_{TET}	70–100%	Energy gap $\Delta E(T_1S - T_1A) \geq 0.1$ eV; triplet lifetime of sensitizer; annihilator concentration; diffusion rate
φ_{TTA}	11–100%	Energy levels T_1, T_2, S_1 of annihilator; high-level reverse ISC (HL-RISC); molecular rigidity
f	5–100%	$f = 2 \cdot \varphi_{TTA}$; maximum 100% if $E(T_2) > 2 \cdot E(T_1) > E(S_1)$
φ_{FL}	30–100%	Steric protection from dimerization and aggregation; substituent electronic effects; heavy-atom effect

The spin-statistical factor f deserves special attention. Classical spin statistics predicts that only 1 of 9 possible spin combinations of two colliding triplets gives a singlet state, so the theoretical maximum would be f = 11% (φ_{UCmax} = 5.5%). However, experimental data have shown this limit is not absolute: for 9,10-diphenylanthracene (DPA), f ≈ 60%, well above 11% [18]. This is explained by high-level reverse intersystem crossing (HL-RISC): the annihilator's T_2 state, which is populated after TTA, can undergo fast radiationless transition to S_1 instead of returning to T_1. The probability of this depends on the energy gap $2 \cdot E(T_1) - E(T_2)$: a larger gap slows internal conversion $T_2 \rightarrow T_1$ and favours the HL-RISC pathway, raising f [17][17]. This is why the relative positions of T_1, T_2 and S_1 in the annihilator are critical design parameters [18].

Another important practical parameter is the threshold excitation intensity I_{th} –the minimum power at which φ^{UC} reaches saturation and the dependence on excitation intensity changes from quadratic to linear. A low I_{th} is desirable for applications under solar irradiance or low-power biological light sources [3].

I.2. High-Performance Annihilators

The choice of annihilator largely determines the efficiency of a TTA-UC system. An ideal annihilator should combine high φ^{FL}, high f factor, a suitable T_1 level for efficient TET from the chosen sensitizer, and good photostability without undesired processes such as singlet fission (SF) or excimer formation. Table 1.2 summarizes the best-reported annihilators by performance category.

Table 1.2. *Selected high-performance annihilators for TTA-UC (50% = theoretical maximum for φ^{UC}).*

Annihilator	φ^{UC}, %	φ^{FL}, %	f, %	Emission	Notes / Ref.
DPA	24.0	~ 100	60	Blue, ~ 430 nm	Benchmark; PtOEP sensitizer [19]
TIPS-Ac	–	~ 80	~ 77 (φ_{TTA})	Blue, ~ 460 nm	NIR-to-blue UC; [20]
Rubrene	~ 5	~ 99	~ 40	Orange, ~ 560 nm	NIR-to-vis; singlet fission in films [5,6]
TIPS-Pyrene	13.7	95	39.2	Green, ~ 490 nm	Record green; PdTPBP sensitizer [13]
Perylene	≤ 9.0	~ 92	17.9	Blue-green, ~ 470 nm	f limited by energy-gap law [9]

DPND	9.4	~ 70	–	NIR, ~ 700 nm	NIR-to-vis; doubles rubrene performance [10]

DPA and its derivatives remain the gold standard for green-to-blue upconversion. The two phenyl groups in the 9,10-positions provide steric shielding that prevents photodimerization and concentration quenching – a known degradation pathway for unprotected anthracenes [21] – while barely affecting the π-system, giving $\varphi^{FL} \approx 100\%$. Rubrene holds the leading position for NIR-to-visible upconversion in the orange region, but its use in solid films is complicated by singlet fission (SF): at high chromophore densities in condensed phases, the S_1 state of rubrene can split into two T_1 states instead of emitting light, severely reducing UC efficiency [5]. Studies of structural modifications to rubrene –including *tert*-butyl substitution and CN-functionalization – have shown that SF can be partially suppressed, enabling better solid-state performance [5,6].

A noteworthy recent contribution is the TIPS-pyrene annihilator, introduced in 2025 [13]. This compound achieves a record green-to-NIR upconversion efficiency of 13.7% (φ^{UC}) together with f = 39.2% and φ^{FL} = 95%. The key finding of that work is that TIPS functionalization *via* an alkynyl linker increases the singlet character of the $^1(T_1T_1)$ excited pair state, which directly raises the probability of singlet formation during TTA – a new design principle applicable to a broad range of annihilator scaffolds [13].

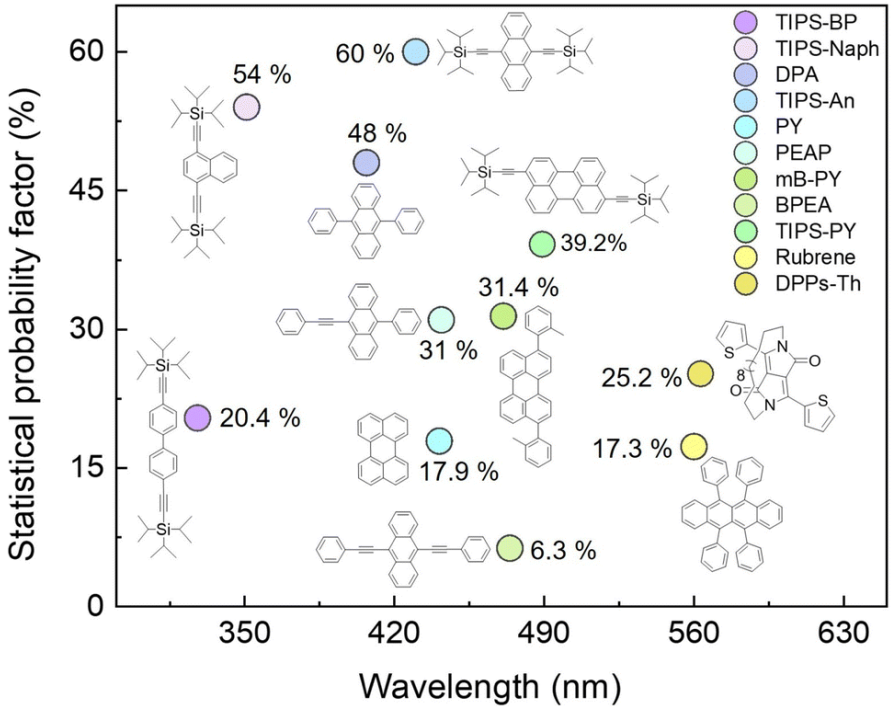

Scheme 1.2. *Observation of various annihilators emitting across the visible spectral range. [13]*

Perylene has long been attractive due to its near-unity fluorescence quantum yield, but its f factor is severely limited by the energy gap law: the small gap between $2 \cdot E(T_1)$ and $E(T_2)$ leads to fast internal conversion $T_2 \rightarrow T_1$ that competes with HL-RISC. A systematic experimental study [9] confirmed $f = 17.9 \pm 2.1\%$ for perylene in THF, setting a practical ceiling of $\varphi^{UC} \approx 9.0\%$ regardless of other optimizations.

I.3. Anthracene Derivatives in TTA-UC

Anthracene and its derivatives play a central role in TTA-UC, combining favourable photophysics with broad chemical tunability. The parent anthracene has $\varphi^{FL} \approx 30\%$ –relatively low because of significant intersystem crossing [22]. However, substitution at the 9,10-positions, which are the most reactive in anthracene, dramatically improves photophysical properties. Even 9,10-dimethylanthracene has $\varphi^{FL} \approx 70\%$ [11], and 9,10-diphenylanthracene (DPA) reaches $\varphi^{FL} \approx 100\%$. The key reason is that bulky 9,10-substituents sterically block the reactive 9,10-bridge from photodimerization and intermolecular π-stacking, which is the main non-radiative quenching pathway [22]. A systematic structure–property study of eight 9,10-disubstituted anthracenes with various donor and acceptor groups showed that UV/Vis absorption and T_1 energies change only slightly with substitution, while fluorescence properties are more sensitive: thiophene-based substituents, for example, lower φ_{FL} to below 10% through spin-orbit coupling enhancement [11].

The main advantages of anthracene derivatives as TTA-UC annihilators are:

1. well-understood photophysics and straightforward structure–property relationships;
2. high φ^{FL} values when appropriate 9,10-substituents are used;
3. favourable energy level arrangement for HL-RISC, giving high f factors;
4. structural flexibility –the 9,10-positions can be functionalized with aryl, alkyl, or alkynyl groups by well-established cross-coupling methods;
5. good thermal and photochemical stability when steric protection is provided.

The limitations include:

1. Emission wavelengths mostly in the blue range (420–490 nm), which limits spectral coverage for some applications;
2. Sensitivity to molecular oxygen, which quenches long-lived triplet states;
3. Tendency to photodimerize and form π-stacks in the absence of sterically protective groups;
4. Variable f factors depending on the exact energy level arrangement.

I.3.1. 9,10-Ethynyl Derivatives of Anthracene

Replacing aryl substituents in the 9,10-positions with alkynyl groups, especially silylethynyl groups, was an important step in the development of anthracene-based annihilators. Several reasons make this class of compounds attractive.

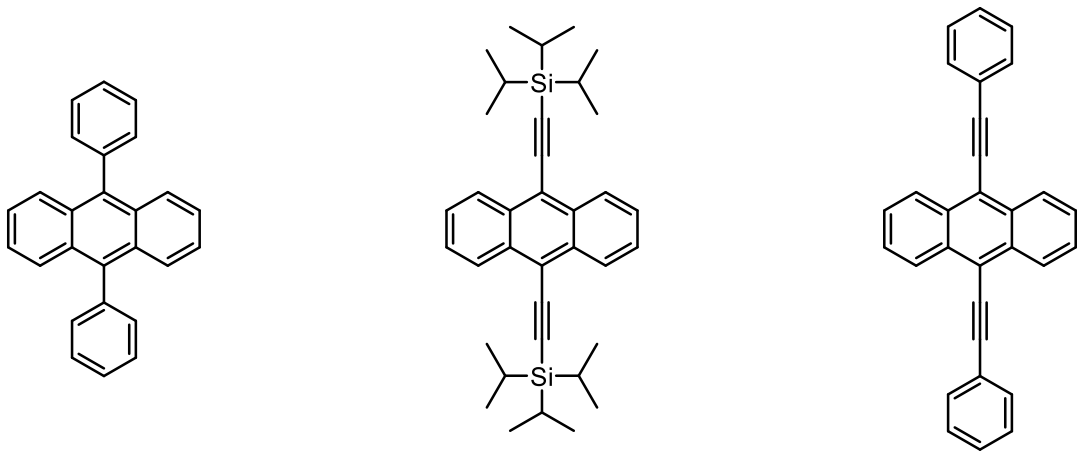

DPA **TIPS-Ac** **BPEA**

Scheme 1.3. *Most common anthracene-based annihilators for TTA UC.*

First, the alkynyl linker R–C≡C–Ant extends the conjugated π-system, causing a bathochromic shift of both absorption and emission relative to unsubstituted anthracene. For 9,10-

bis(triisopropylsilylethynyl)anthracene (TIPS-Ac), emission is shifted to 450 – 490 nm. This improves the energy match with long-wavelength sensitizers and extends the accessible anti-Stokes shift [20].

Second, bulky trialkyl- or triarylsilyl groups attached at the end of the alkyne linker provide effective steric shielding of the anthracene core against photodimerization and π-aggregation –the same protective effect as phenyl groups in DPA, but with additional spectral tunability [22].

Third, silicon and related group-14 elements in silyl groups exert a specific electronic effect on the π-system through σ–π* hyperconjugation: the Si–C σ* orbital mixes with the aromatic π-system, stabilizing the S_1 state and reducing the non-radiative rate constant k_{nr}, which raises φ^{FL}. This effect has been documented for a broad range of silylethynyl arenes - for example, TIPS-substituted pyrenes show φ_{FL} values up to 0.99, far above unsubstituted pyrene (0.32) [13].

TIPS-Ac is now a commercially available annihilator and one of the most well-studied compounds for NIR-to-blue TTA-UC. A landmark study published in 2019 [20] demonstrated efficient NIR-to-blue upconversion using TIPS-Ac with a relatively small driving force for TET (<0.32 eV), achieving φ^{TTA} = 77 ± 3%. This opened the way for anthracene-based systems with large anti-Stokes shifts operating within the biological transparency window (700–900 nm), relevant for biomedical imaging and photocatalysis [20].

Table 1.3. *Summary of 9,10-diethynylanthracene derivatives and their TTA-UC performance. *φ^{UC} not reported due to different sensitizer system.*

Compound	φ^{FL}, %	Emission, nm	φ^{UC}, %	Notes / Ref.
DPA	~100	~430	24.0	Benchmark; PtOEP [11,19]
TIPS-Ac	~80	460–490	N/A*	φ^{TTA} = 77%; NIR-to-blue [20]
BPEA	~85	~490	~2–3	Low f ≈ 6%; green emitter [17]

I.4. Synthetic Methods for 9,10-Diethynylanthracenes

I.4.1. Sonogashira Cross-Coupling

The Sonogashira reaction – palladium-catalyzed coupling of an aryl halide with a terminal alkyne –is the most widely used route to 9,10-diethynylanthracenes [23]. The aryl substrate is typically 9,10-dibromoanthracene, which is readily available either by direct bromination of anthracene or by reduction of anthracene-9,10-dione followed by halogenation.

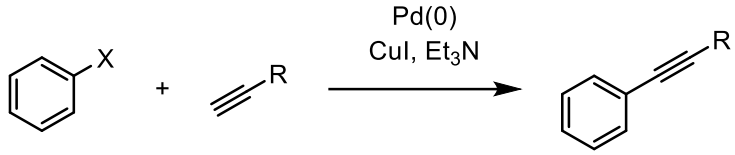

Scheme 1.4. *Sonogashira coupling reaction scheme.*

Standard conditions use $Pd(PPh_3)_2Cl_2$ (5–10 mol%), CuI (10–40 mol%), Et_3N or iPr_2NH as base, 70–80 °C, 12–24 h. For non-volatile, crystalline alkynes, isolated yields are typically 70–90% [23,24]. Microwave irradiation significantly shortens reaction times to 1–2 hours at higher temperatures (100–140 °C) with comparable or better yields, and in some cases allows product isolation by simple recrystallization without column chromatography [24].

Key limitations of the method include: (1) volatile alkynes gradually evaporate from the reaction mixture, reducing yields and requiring temperature adjustments; (2) terminal diynes and other reactive alkynes may undergo copper-mediated homocoupling (Glaser conditions), leading to oligomerization; (3) tin-containing alkynes can react under Stille-type pathways, giving terminal diynes instead of the expected coupling product [23,12]

Copper-free Sonogashira protocols, which use $Pd_2(dba)_3$ with phosphine ligands in amide solvents, can reduce homocoupling but at the cost of more complex catalyst systems and different substrate scope [12].

I.4.2. Lithium Acetylide Addition

When a terminal alkyne is incompatible with palladium-catalyzed conditions, the corresponding lithium acetylide (formed by treatment with *n*-BuLi at −78 °C) can be added to an electrophilic chlorosilane, chlorogermane, or chlorostannane to give the desired product [12]. This method is particularly valuable for organotin and organogermanium substituents.

Steric bulk of the electrophile is the key limiting factor: while less hindered substrates such as Et_3GeCl and Ph_3SiCl react in reasonable yields (58% and 54%, respectively, in this work), bulkier electrophiles such as adamantyl chloride (AdCl) and tin chlorides (Bu_3SnCl, Me_3SnCl) give traces of product or fail completely. Addition of HMPA as a co-solvent, which increases the reactivity of organolithium species by coordinating to lithium, improved results for tributyltin chloride only marginally [12].

I.4.3. Anthraquinone Reduction Route

A classical approach to 9,10-substituted anthracenes involves addition of organometallic reagents (aryl Grignard or arylboronic acids via Suzuki coupling) to anthracene-9,10-dione, followed by reductive aromatization. The resulting 9,10-diaryl-9,10-dihydroanthracene-9,10-diol intermediates are reduced with $SnCl_2$ or KI/NaH_2PO_2 in AcOH to give the fully aromatic product [12]. This method is well established for aryl substituents (e.g., DPA) but is not directly applicable to alkynyl groups because terminal alkynyl organometallics are typically not stable enough under these conditions.

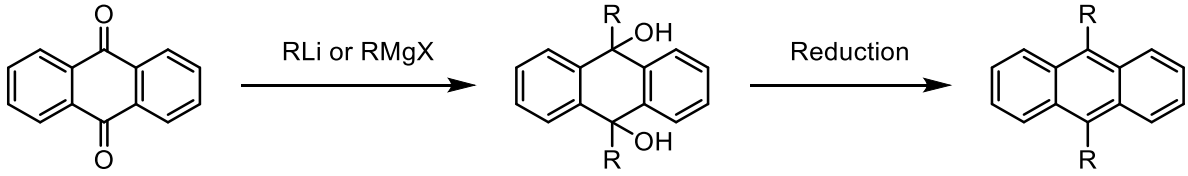

Scheme 1.5. *Anthracene derivatives synthesis via anthraquinone.*

For arylethynyl substituents (e.g., BPEA), a modified route involves addition of arylethynyl Grignard reagents to anthraquinone, followed by $SnBr_2$-mediated reduction of the diol intermediate. This is a viable multi-step alternative when 9,10-dibromoanthracene is not easily available [12].

I.5. Applications of TTA-UC

Table 1.4. *Main application areas of TTA-UC and the role of anthracene-based annihilators.*

Application area	Role of TTA-UC	Role of anthracene derivatives	Refs.

Solar cells	Convert sub-bandgap NIR photons into visible photons absorbed by the cell	DPA and TIPS-Ac used as annihilators in UC layers placed below solar cells;	[25,26]
Bioimaging	NIR excitation to blue/violet emission for cell and tissue imaging with low autofluorescence	DPA/PtOEP in silica and PLGA nanoparticles used for lymph node and tumour imaging in mice;	[7,8]
Photodynamic therapy	Upconverted photons activate photosensitizers deep in tissue	Anthracene nanoparticles proposed as UC agents for NIR-activated PDT;	[8]
OLED	TTA-based delayed fluorescence boosts EQE beyond the 25% singlet limit	DPA derivatives studied as blue emitters in TTA-OLEDs; emission ~440 nm;	[33]
Photocatalysis	Upconverted UV/visible light drives reactions that normally need UV excitation	TIPS-Ac used in NIR-driven C–O bond formation; DPA NPs used in photobiocatalysis.	[28,29]

Solar energy harvesting is one of the most studied potential applications of TTA-UC. According to the Shockley–Queisser limit, single-junction solar cells cannot use photons with energy below the semiconductor bandgap [30,25]. A TTA-UC layer placed behind the cell can convert these sub-bandgap photons to higher-energy photons that the cell can absorb, theoretically increasing efficiency by up to 30%. Experiments with dye-sensitized solar cells (DSSC) integrated with rubrene-based UC layers have demonstrated measurable increases in short-circuit current density ($\Delta Jsc = 1.65$ mA/cm^2) under monochromatic 635 nm excitation at 1 sun intensity [26]. DPA and TIPS-Ac have also been studied as annihilators in UC systems paired with perovskite nanocrystal sensitizers, where a composite DPA+TIPS-Ac annihilator system showed more than five-fold enhancement in upconversion yield [29].

For bioimaging, organic TTA-UC nanoparticles based on anthracene annihilators are particularly interesting. They can be excited by NIR light (700–900 nm) –wavelengths that penetrate several centimetres into biological tissue –while emitting in the blue range (430–490 nm). This provides high signal-to-noise ratio because biological autofluorescence is negligible at these emission wavelengths. DPA/PtOEP nanoparticles encapsulated in silica gave $\varphi^{UC} = 4.5\%$ in aqueous solution under air-equilibrated conditions, and were successfully used for *in vivo* lymph node imaging in mice [7]. More recently, PLGA-encapsulated DPA/PtOEP nanoparticles were applied to imaging excised tumour cryosections from mice with injected nanoparticles [8].

For photocatalysis, TIPS-Ac was used in 2024 as the annihilator in a dual nickel/photoredox catalytic system for C–O bond formation under NIR irradiation: the upconverted blue photons generated *in situ* drove the photoredox step that is normally not accessible with green or red light

[28]. DPA/PtOEP nanoparticles were also used to broaden the wavelength range for photobiocatalysis, activating flavin-dependent photoenzymes with upconverted photons [29].

II. RESULTS AND DISCUSSION

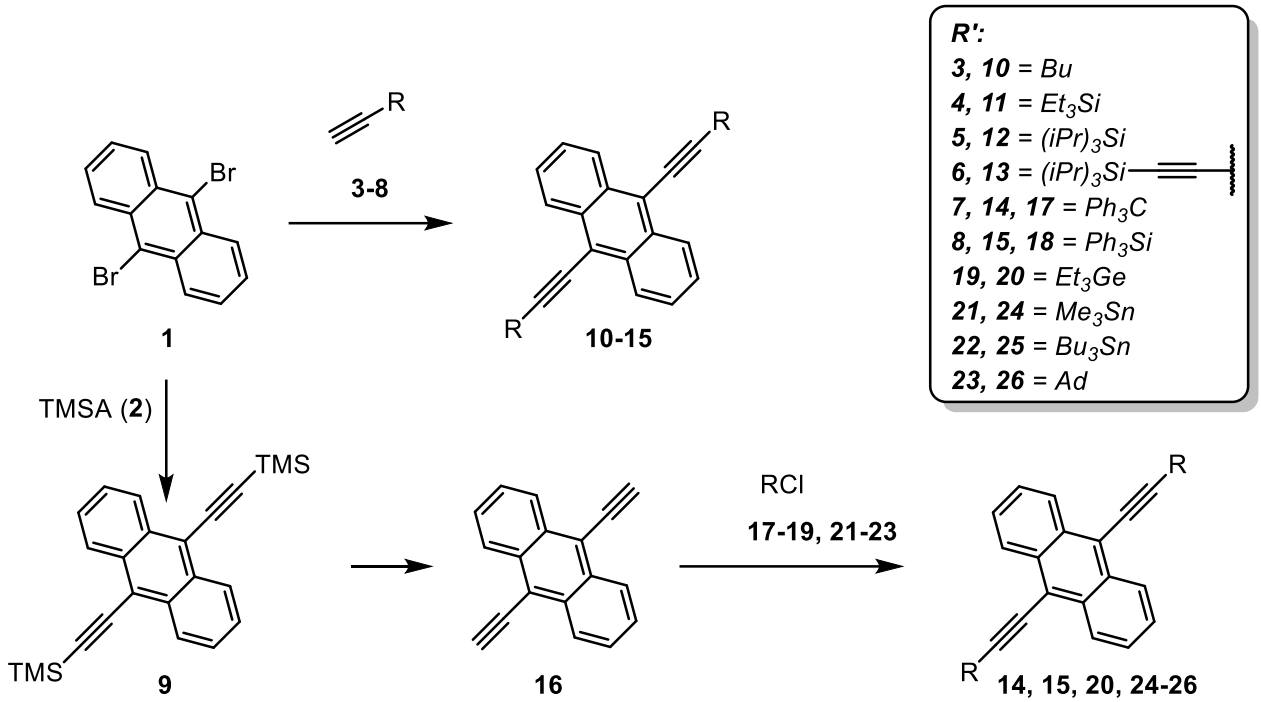

Scheme 2.1. *Synthetic roots for anthracene derivatives used in this work.*

In this work, a series of 9,10-diethynylanthracene derivatives (**9**, **10 – 15**, and **20**) bearing structurally diverse substituents were synthesized in moderate to excellent yields (Scheme 2.1 and 2.2). Three target compounds –the trimethyltin- (**24**), tributyltin- (**25**) and adamantyl-substituted (**26**) derivatives –could not be obtained in sufficient purity or quantity; these cases are discussed separately below.

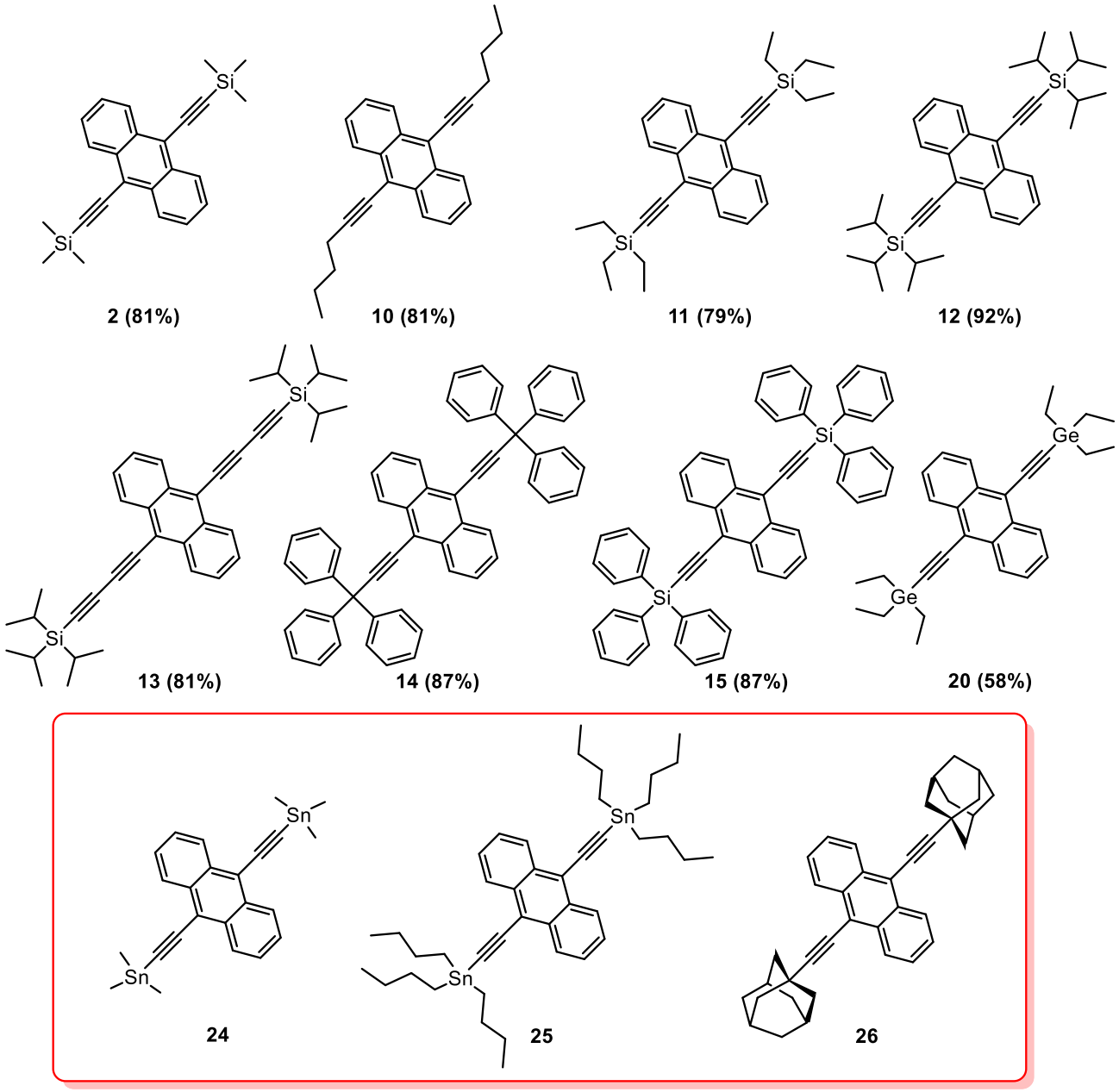

Scheme 2.2. *List of 9,10-diethynylanthracenes with yields. (In red frame – substances not obtained)*

II.1. Sonogashira Coupling

To optimize the Sonogashira coupling of 9,10-dibromoanthracene (**1**) with a range of alkynes, reaction conditions were systematically evaluated (Scheme 2.3, Table 2.1). All experiments used an identical catalyst system showed in Scheme 2.2.

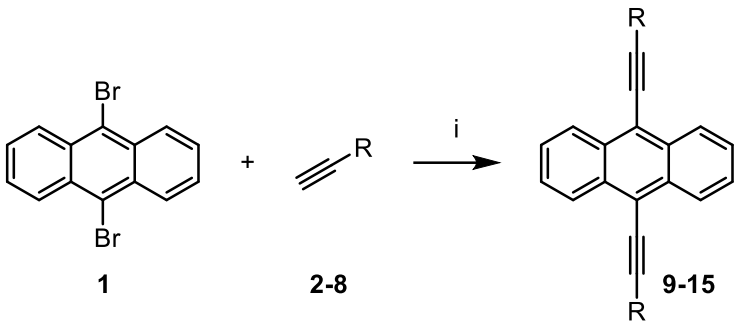

Scheme *2.3.* *Reagents and conditions:* (i) ArBr (1 eq.), alkyne (4 eq.), Et_3N, $Pd(PPh_3)_2Cl_2$ (10 mol%), PPh_3 (20 mol%), CuI (40 mol%), Ar, heat.

Table 2.1. *Sonogashira coupling reactions. Bold rows – best conditions per substrate. MW = microwave irradiation.*

Alkyne	MW irradiation	T, °C	Time, h	Result	Yield[1], %	Product №
Me_3Si—≡ **2**	×	80	16	Partial conversion	-	**9**
	×	80	24	Partial conversion	77	
	✓	80	2	Partial conversion	-	
	✓	100	2	Partial conversion	81	
Bu—≡ **3**	×	80	16	Partial conversion	-	**10**
	×	80	24	Partial conversion	81	
	✓	100	2	Partial conversion	72	
	✓	140	0.5	Decomposed	0	
$(iPr)_3Si$—≡ **5**	×	80	16	Partial conversion	64	**12**
	×	80	24	Partial conversion	79	
	✓	**120**	**1**	**Completed**	**92**	
Ph_3Si—≡ **8**	×	80	24	Partial conversion	52	**15**
	✓	**120**	**1**	**Completed**	**87**	
Et_3Si—≡ **4**	×	80	16	Partial conversion	79	**11**
$(iPr)_3Si$—≡—≡ **6**	×	80	16	Partial conversion	81	**13**
Ph_3C—≡ **7**	×	80	16	Partial conversion	83	**14**

The results show a clear dependence on the physical properties of the alkyne substrate. Reactions with volatile alkynes (**2** and **3**) proceeded slower than those with non-volatile or crystalline reagents, most likely because the alkyne gradually evaporated from the reaction mixture. The synthesis temperature was reduced in these cases to improve yield. Microwave-

[1] Total yield after isolation and purification by column chromatography or/and recrystallization.

assisted synthesis proved significantly better across the series: reaction times were reduced from 16–24 hours to 1–2 hours, and in several cases –most notably for TIPS-acetylene (**5**) and ethynyltriphenylsilane (**8**) –excellent yields were achieved with high enough purity to allow isolation by simple recrystallization without column chromatography. These results show good potential for further optimization of Sonogashira conditions for this substrate class.

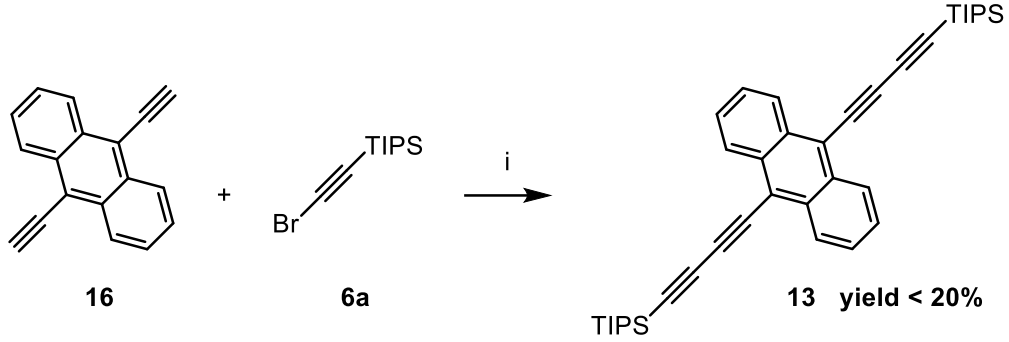

Scheme 2.4. *Reagents and conditions:* **16** (1 eq.), bromoalkyne **6a** (4 eq.), Et_3N, $Pd(PPh_3)_2Cl_2$ (10 mol%), PPh_3 (20 mol%), CuI (40 mol%), Ar, 80 °C, 16 h.

An attempt was also made to use the terminal diyne **16** and bromoalkyne **6a** as substrates (Scheme 2.4). Under both conventional and microwave conditions, the target product was obtained in less than 20% yield. The formation of a red precipitate strongly suggests alkyne oligomerization as the main competing pathway, consistent with the known tendency of terminal diynes to undergo copper-mediated homocoupling (Glaser reaction) under these conditions.

II.2. Lithium Acetylide Synthesis and Nucleophilic Substitution

For substrates incompatible with Sonogashira conditions, an alternative route via lithium acetylide intermediates was used (Scheme 2.5, Table 2.2). This was necessary because certain alkynes were not stable under palladium-catalyzed conditions: for example, the tin-containing alkyne gave the terminal diyne as the major product rather than the desired cross-coupling adduct.

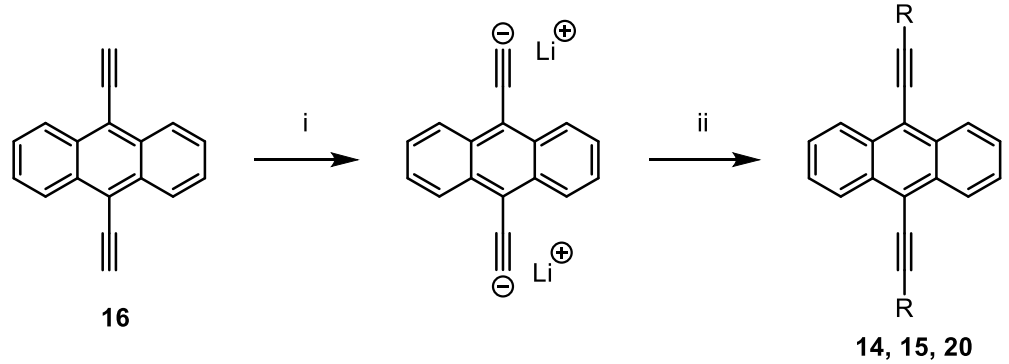

Scheme 2.5. *Reagents and conditions:* (i) **16** (1 eq.), *n*-BuLi (3 eq.), THF, -78 °C, Ar, 0.5 h; (ii) RCl (4-6 eq.), THF, -78→20°C, Ar, 2 – 16 h.

Table 2.2. *Nucleophilic substitution via lithium acetylides.*

RCl	Time, h	Result	Yield[2], %	Product №
Ph_3CCl (**17**)	24	Partial conversion	traces	**14**
Ph_3SiCl (18)	**24**	**Partial conversion**	**54**	**15**

[2] Total yield after isolation and purification by column chromatography or/and recrystallization.

Et_3GeCl (19)	**2**	**Completed**	**58**	**20**
Me_3SnCl (**21**)	24	No result	0	**24**
Bu_3SnCl (**22**)	24	Partial conversion	traces	**25**
AdCl (**23**)	24	No result	0	**26**

The results in Table 2.2 show a clear dependence on the steric demand of the electrophile. Reactions with less bulky chlorogermanes and chlorosilanes went well: Et_3GeCl gave compound **20** in 58% yield with complete conversion after only 2 hours, and Ph_3SiCl gave compound **15** in 54% yield. In contrast, the much bulkier trityl chloride (Ph_3CCl) gave only traces of compound **14**, while both tin chlorides failed to give any isolable product. These results point to a steric effect at the electrophilic carbon that becomes the main barrier beyond a certain size threshold. The failure of tin chlorides also suggests that product instability - for example, protodestannylation - may be a competing problem, not just slow reaction.

II.3. Synthesis of Tin-Containing Anthracene Derivatives

The synthesis of tin-substituted anthracene derivatives was the most difficult part of this work. Despite many attempts to optimize conditions, no pure product could be isolated at the time of writing (Table 2.3). Under standard lithiation conditions (*n*-BuLi, THF, −78 → 20 °C), neither Me_3SnCl nor Bu_3SnCl gave any product. Adding HMPA as a co-solvent –which increases the reactivity of organolithium species –helped only slightly with Bu_3SnCl and not at all with Me_3SnCl. Using LDA instead of *n*-BuLi, or raising the temperature to 60 °C with HMPA, also failed. An alternative approach using $(Bu_3Sn)_2O$ as a neutral tin source gave no product under thermal conditions. A fluoride-mediated route (TBAF desilylation of TMS-protected precursors **9** and **12** followed by trapping with $(Bu_3Sn)_2O$) showed partial conversion, but purification was not possible at this stage.

The fact that all these mechanistically different approaches failed suggests the problem is not in generating the acetylide nucleophile, but in the instability of the stannylated product under the reaction conditions. Protodestannylation or competitive reduction of the tin electrophile are likely pathways that need further investigation.

Table 2.3. *Tin-derivatives syntheses*

Substrate	Alkyne №	Reagents	T, °C	Time, h	Result
Me_3SnCl	**16**	*n*-BuLi, THF	-78→20	24	-
		n-BuLi, HMPA, THF		24	-
		LDA, THF		24	-
Bu_3SnCl	**16**	*n*-BuLi, THF	-78→20	24	-
		n-BuLi, HMPA, THF		24	traces
		LDA*, THF		24	traces
		n-BuLi, HMPA, THF	60	2	traces

	16	toluene	90	3	-
$(Bu_3Sn)_2O$	**9**	$TBAF_{20\%}$, THF	0	1	Partial conversion
	12	$TBAF_{20\%}$, THF	60	1	(bad purification)

* LDA was prepared *in situ* from $(i\text{Pr})_2\text{NH}$ and nBuLi. Then it was used for preparation of $Bu_3SnN(i\text{Pr})_2$[31].

II.4. Synthesis of the Adamantyl Derivative

Since adamantyl chloride could not be used in the lithiation–substitution route (Table 2.2), two alternative strategies were tried for introducing the adamantyl group (Scheme 2.6, Table 2.4). The Grignard approach –reacting ethynylmagnesium bromide with an adamantyl electrophile in toluene at 110 °C –gave no detectable product. Treatment with trimethylsilylacetylene (TMSA) with $AlCl_3$ (30 mol%) as a Lewis acid at low temperature gave only traces of the target compound. Attempts to use compound **9** (9,10-bis(TMS-ethynyl)anthracene) as the acetylene source under the same Lewis acid conditions gave unidentified black or gray solids at both 0 and −45 °C, pointing to decomposition or polymerization of the anthracene core instead of clean substitution.

These results together suggest that electrophilic substitution at the bridgehead carbon of adamantane is not feasible under any of the conditions tested. This is likely due to the combination of strong steric shielding at the bridgehead position and low reactivity of the available leaving groups. An alternative synthetic strategy –building the adamantyl–alkyne bond before attaching to the anthracene –may be a better approach for this target.

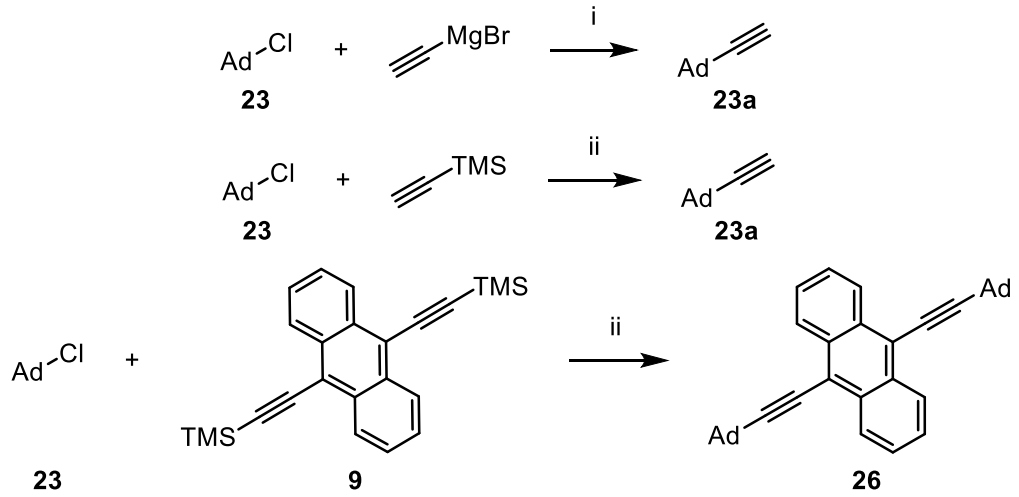

Scheme 2.6. *Reagents and conditions:* (i) toluene, reflux, Ar, 16 h; (ii) $AlCl_3$ (30 mol%), CH_2Cl_2, Ar, -45 °C, 2h.

Table 2.4.

Reagent	Conditions	Result
Ethynylmagnesium bromide	110 °C, 16 h	-
TMSA	0 °C, 2 h	traces
9,10-Bis((trimethylsilyl)ethynyl)anthracene	0 °C, 2 h	Black solid, unidentified (mix)
	-45 °C, 2 h	Gray solid, unidentified (mix)

II.5. Photophysical Properties and Upconversion Performance

The photophysical properties of selected synthesized 9,10-diethynylanthracene derivatives were evaluated as annihilators in TTA-UC systems in THF solution, using PtOEP as the sensitizer. The key parameters –upconversion quantum yield (φ_{UC}), fluorescence quantum yield (φ_{FL}), TTA efficiency (φ_{TTA}), and spin-statistical factor *f* –are collected in Table 2.5. Across the whole series, all compounds show quantitative ISC in the sensitizer (φ_{ISC} = 100%) and near-quantitative triplet energy transfer to the annihilator (φ_{TET} = 99–100%), confirming that triplet sensitization is efficient and not the limiting step. The main differences in performance come from variations in φ_{FL}, φ_{TTA}, and the spin-statistical factor *f*.

Table 2.5. *Parameters of UC samples in THF (c[A] = 2mM, c[PtOEP] = 20 μM. UCQY and FLQY calculated with S spectrum from diluted solution. Measured by Manvydas Dapkevičius; c[A] = 0.1 mM, c[PdTPBP] = 10 μM*. Measured by Manvydas Dapkevičius; c[A] = 10 mM, c[PtOEP] = 10 μM**.*

Annihilator	ϕ_{UC}^{∞} (%)	ϕ_{UC} (%)	ϕ_{FL_ED} (%)	ϕ_{ISC} (%)	ϕ_{TET} (%)	ϕ_{TTA} (%)	f (%)
bPhE(TB)-Anc (BPEA)*	3.1	2.7	81.6	100	95	100	7.9
PhE-TIPS(TB)-Anc	11.6	7.8	40.2	100	99.7	66.8	58.1
bSiSi(TB)-Anc	9.8	7.3	33.3	100	99.0	74.5	59.6
bTPhS(TB)-Anc	19.4	18.3	58.6	100	99.5	94.7	66.4
bTIPS(bTB)-Anc	-	-	-	-	-	-	-
bTIPS(TB)-Anc (E.O.)	18.1	14.8	56.4	100	99.6	82.1	64.3
bTIPS(TB)-Anc (Old)	16.3	13.9	56.7	100	99.6	85.0	57.8
bTIPS(TB)-Anc (J.L.)	21.9	20.6	70.8	100	98.8	94.1	62.7

bTEGe(TB)-Anc	15.6	12.2	54.6	100	99.5	78.4	57.3
bTESi(TB)-Anc	-	-	-	-	-	-	-
bTPhC(TB)-Anc	**26.7**	**25.5**	**66.5**	**100**	**99.3**	**95.5**	**80.9**
Ph-TIPS(TB)-Anc	11.4	8.3	57.2	100	99.6	72.9	40.1
bTPhS(DB)-Anc	0.26	0.16	46.1	100	99.3	61.5	1.1
Ph-TPhS(DB)-Anc	6.1	4.7	27.0	100	99.6	77.4	45.5
bPh-Anc (DPA)**	24.0	24.0	79.9	100	100	100	60
Anc	-	-	-	-	-	-	-

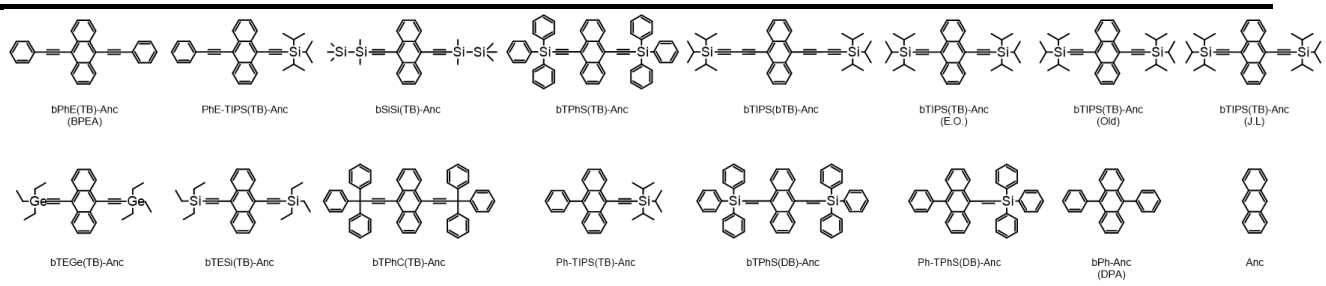

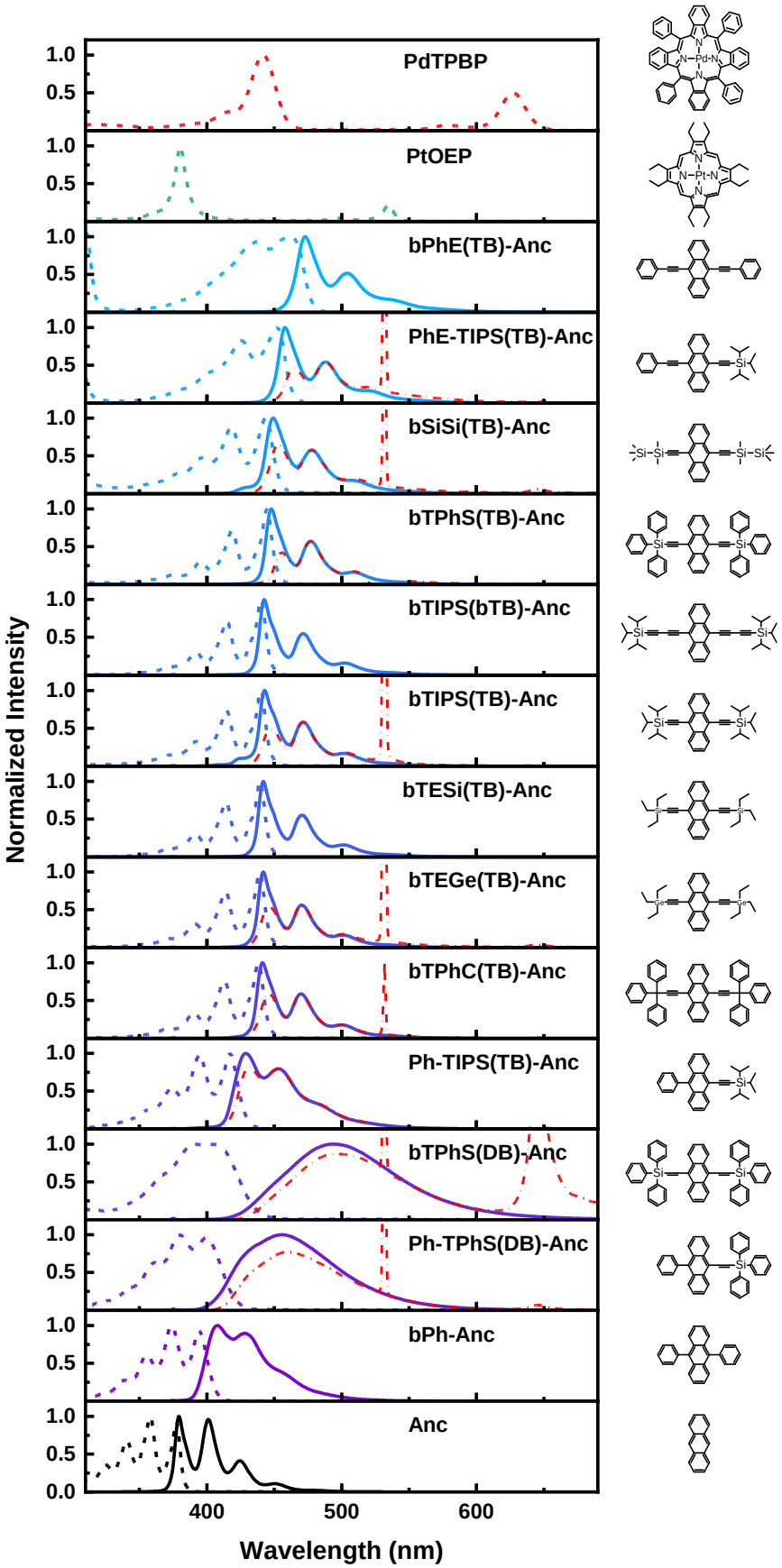

Fig.2.1. *Normalized absorbtion (dashed lines) and fluorescence (solid lines) spectra of sensitizers and annihilators in THF (c = 0.01 mM). Dash dot lines represent UC spectra (excited with 532 nm DPSS CW laser). bTPhS(TB)-Anc and Ph-TIPS(TB)-Anc UC spectra were measured with 532 nm notch filter.*

The best upconversion performance in this study was achieved by bTPhC(TB)-Anc (compound **14**), which bears trityl (triphenylmethyl) substituents. It gave φ_{UC} = 25.5% with f = 80.9%, closely matching the reference annihilator DPA (φ_{UC} = 24.0%, f = 60%) and actually surpassing it in TTA efficiency (φ_{TTA} = 95.5% vs. 100% for DPA). This is a notable result given that the trityl group introduces a sp^3-hybridized carbon at the attachment point, which means there is no conjugation between the substituent and the anthracene core. The steric bulk of three phenyl rings around the sp^3 carbon appears to be the key factor: it shields the anthracene face from intermolecular contacts, preventing concentration quenching and photodimerization [5]. Because the trityl carbon is sp^3, it does not perturb the anthracene π-system, so φ_{FL} stays at a useful 66.5%. The combination of good steric protection and minimal electronic perturbation explains the outstanding performance.

Compound **12**-based bTIPS(TB)-Anc was tested in three independently prepared batches and gave φ_{UC} values of 13.9–20.6%, with the best batch reaching φ_{UC} = 20.6% and f = 62.7%. The TIPS group is attached *via* an alkyne linker and exerts a σ-donating electronic effect through silicon, which is known to raise φ_{FL} in silylethynyl-substituted acenes by lowering the non-radiative rate [13]. The variation between batches is notable: the best batch (J.L.) had φ_{FL} = 70.8%, significantly higher than the others (~56%), which shows sensitivity of this compound to purity.

Replacing silicon with germanium in compound **20** (bTEGe(TB)-Anc, triethylgermyl substituent) gives a moderate decrease in performance (φ_{UC} = 12.2% vs. ~14–20% for TIPS). This is consistent with the heavy-atom effect: germanium has larger spin-orbit coupling than silicon, which can speed up ISC from the excited singlet, reducing φ_{FL} (54.6% for **20** vs. 56–71% for TIPS batches). The effect is moderate at the Si/Ge level but is visible in the data.

Compound **15** bearing triphenylsilyl groups (bTPhS(TB)-Anc, φ_{UC} = 18.3%) performs better than most TIPS batches, which might seem surprising since larger aromatic groups on silicon are reported to introduce extra non-radiative decay channels in some annihilator families. [13]

In the anthracene series studied here, the phenyl groups on silicon apparently do not cause significant deactivation, possibly because the electronic perturbation from Si–Ph conjugation is directed away from the anthracene π-system.

Extending the alkyne spacer to a diyne unit in bTIPS(bTB)-Anc **13** gave no measurable upconversion. This is consistent with the bathochromic shift expected from extended conjugation through multiple triple bonds, which lowers T_1 of the annihilator and may bring it outside the efficient Dexter transfer window from PtOEP. The doubly bridged (DB) anthracene derivatives bTPhS(DB)-Anc and Ph-TPhS(DB)-Anc showed a dramatic drop in φ_{UC} to 0.16% and 4.7%, respectively. Their absorption and emission spectra are significantly red-shifted and broadened compared to the TB series (Fig. 2.1), indicating strong perturbation of the anthracene π-system by the double bridge. This reduces the anti-Stokes shift available for upconversion and likely increases non-radiative decay rates.

III. EXPERIMENTAL PART

III.1. Instrumentation

Melting points were determined in open capillaries using a digital melting point IA9100 series apparatus (Thermo Fisher Scientific) and are uncorrected.

Microwave Synthesis Reactor "Monowave 300", 850 kW, 1200 rpm.

^{1}H and ^{13}C NMR spectra were recorded on a „Bruker Ascend 400" (400 MHz and 100 MHz, respectively)

The following abbreviations are used for ^{1}H NMR multiplicities: s = singlet; d = doublet; dd = doublet of doublets; t = triplet; td = triplet of doublets; q = quartet; p = quintet; hex = sextet; m = multiplet.

All reactions were monitored by TLC using Silica Gel 60 F_{254} aluminium plates (Merck). Visualization was performed under UV light (254 nm and 365 nm). Column chromatography was carried out with Silica Gel 60 (0.040–0.063 mm, Merck).

All reactions were performed under an inert argon atmosphere.

III.2. Materials

General method A. The Sonogashira coupling.

Mixture of 9,10-dibromoanthracene (**1**) (1 eq.), $Pd(PPh_3)_2Cl_2$ (10 mol%), PPh_3 (20 mol%), CuI (40 mol%) in anhydrous Et_3N was flushed with argon. After 5 minutes appropriate alkyne (4 eq.) was added under argon flow. The reaction mixture was stirred at 80 °C for 16 hours. Then aq. NH_4Cl was added and solution was extracted with chloroform. Organic fractions were combined, washed with brine and dried over Na_2SO_4. Chloroform was removed under reduced pressure and the residue was purified by column chromatography on silica gel using petroleum ether.

General method B. Microwave synthesis

Mixture of 9,10-dibromoanthracene (**1**) (1 eq.), $Pd(PPh_3)_2Cl_2$ (10 mol%), PPh_3 (20 mol%), CuI (40 mol%) in anhydrous Et_3N was flushed with argon. After 5 minutes appropriate alkyne (4 eq.) was added under argon flow. The reaction mixture was stirred at 120 °C for 0.5-2 hours in microwave (monitored by TLC). Then aq. NH_4Cl was added and solution was extracted with chloroform. Organic fractions were combined, washed with brine and dried over Na_2SO_4. Chloroform was removed under reduced pressure and the residue was purified by column chromatography on silica using petroleum ether.

*9,10-Bis((trimethylsilyl)ethynyl)anthracene (**9**)*

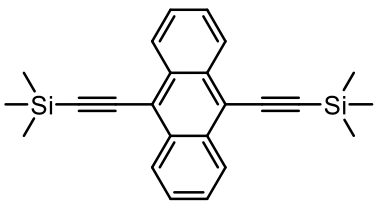

Method I. According to **general method A**, the Sonogashira coupling was carried out with (trimethylsilyl)acetylene (**2**) as appropriate alkyne. The obtained product (**9**) was purified by column chromatography (petroleum ether) and obtained as a red solid (0.844 g, 77%). The spectral characteristics correspond to literature data.

Method II. According to **general method B**, the Sonogashira coupling was carried out with (trimethylsilyl)acetylene (**2**) in microwave at 100 °C for 2 hours. The obtained product (**9**) was purified by column chromatography (petroleum ether) and obtained as a red solid (yield 81%).

*9,10-Diethynylanthracene (**16**)*

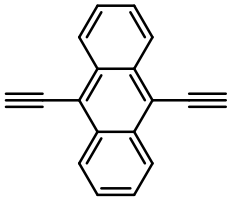

To compound (**9**) in THF/methanol (1:1) solution (0.8 g, 2.16 mmol, 1 eq.) under argon was added KOH powder (0.485 g, 8.64 mmol, 4 eq.). The mixture was stirred for 16 hours at 20 °C. Then solution was poured in H_2O, extracted with Et_2O. Combined organic layers were washed with brine and dried over $MgSO_4$. Solvent was removed under reduced pressure and obtained residue was purified by column chromatography (petroleum ether), giving brownish-yellow solid (**16**) (0.474 g, 97%), that was used immediately. ^{1}H NMR (400 MHz, $CDCl_3$) δ 8.45 (dd, *J* = 6.7, 3.3 Hz, 4H), 7.46 (dd, *J* = 6.7, 3.2 Hz, 4H), 3.91 (s, 2H).

*9,10-Di(hex-1-yn-1-yl)anthracene (**10**)*

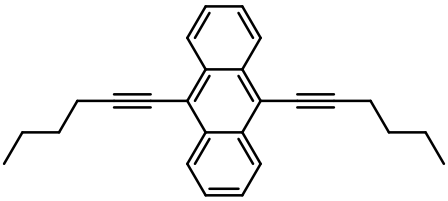

Compound (**10**) was prepared according to **general method A** with hex-1-yne (**3**) as appropriate alkyne. Brownish solid (yield 81%). M.p. 84 – 86 °C. ^{1}H NMR (400 MHz, $CDCl_3$) δ 8.37 (dd, *J* = 6.7, 3.3 Hz, 4H), 7.37 (dd, *J* = 6.7, 3.3 Hz, 4H), 2.57 (t, *J* = 7.1 Hz, 4H), 1.61 (p, *J* = 7.2 Hz, 4H), 1.45 (hex, *J* = 7.3 Hz, 4H), 0.84 (td, *J* = 7.3, 1.2 Hz, 6H). ^{13}C NMR (100 MHz, $CDCl_3$) δ 132.1, 127.3, 126.3, 118.6, 103.3, 77.41, 31.2, 22.3, 19.97, 13.8.

*Triethyl(ethynyl)silane (**4**)*

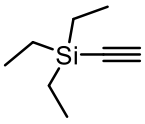

To solution of triethylchlorosilane (0.45 ml, 0.404 g, 2.68 mmol, 1 eq.) in anhydrous THF under argon was added ethynylmagnesium bromide (0.5 M solution in THF, 13 ml, 6.70 mmol, 2.5 eq.). Mixture was stirred under reflux for 5 hours. Then the solution was cooled, quenched with cold aq. NH_4Cl and extracted with CH_2Cl_2. Combined organic layers were washed with brine and dried over Na_2SO_4. Solvent was removed under reduced pressure and residue was purified by column chromatography on silica using petroleum ether. (Triethylsilyl)acetylene (**4**) (0.323 g, 86%) was obtained as colourless liquid and used immediately after purification.

*9,10-Bis((triethylsilyl)ethynyl)anthracene (**11**)*

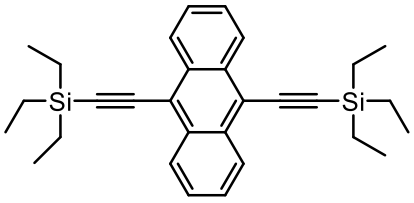

According to **general method A**, the Sonogashira coupling was carried out with (**4a**) as appropriate alkyne. The obtained product was purified by column chromatography (petroleum ether/ethyl acetate 95:5) and recrystallized from toluene/methanol as a yellow solid (**11**) (yield 79%). M.p. 118 – 119 °C. ^{1}H NMR (400 MHz, $CDCl_3$) δ 8.60 (dd, *J* = 6.7, 3.3 Hz, 4H), 7.59 (dd, *J* = 6.7, 3.3 Hz, 4H), 1.17 (t, *J* = 7.9 Hz, 18H), 0.87 – 0.79 (m, 12H). ^{13}C NMR (100 MHz, $CDCl_3$) δ 132.4, 127.3, 126.9, 118.7, 105.9, 102.7, 7.8, 4.7.

*9,10-Bis((triethylgermyl)ethynyl)anthracene (**20**)*

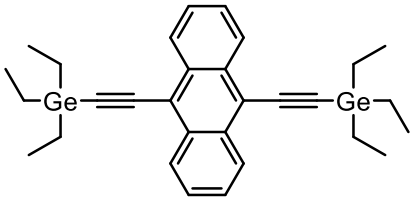

A flame dry round bottom flask covered with septum was purged with argon. Then (**16**) (0.1 g, 0.44 mmol, 1 eq.) in dry THF was added and solution was cooled to -78 °C under argon. *n*-BuLi (2.5 M in hexanes, 0.531 ml, 1.33 mmol, 3 eq.) was added dropwise. The solution was stirred under argon 0.5 h at -78 °C and then triethylchlorogerman (0.441 ml, 0.518 g, 2.65 mmol, 6 eq.) in dry THF was added dropwise. The reaction mixture was slowly warmed to room temperature and stirred for 2 hours. Solution was quenched with cold water, extracted with Et_2O. Organic phase was washed with brine and dried over $MgSO_4$. After that solvent was removed under reduced pressure. Residue was purified by column chromatography (petroleum ether) and recrystallized in toluene/methanol as an orange solid (**20**) (0.14 g, 58%). M.p. 139 – 140 °C. ^{1}H NMR (400 MHz, $CDCl_3$) δ 8.44 (dd, *J* = 6.7, 3.3 Hz, 4H), 7.39 (dd, *J* = 6.7, 3.3 Hz, 4H), 1.09 (td, *J* = 7.8, 0.7 Hz, 18H), 0.90 (qd, *J* = 7.7, 1.2 Hz, 12H). ^{13}C NMR (100 MHz, $CDCl_3$) δ 132.3, 127.4, 126.6, 118.7, 106.4, 102.3, 9.3, 6.1.

*9,10-Bis((triisopropylsilyl)ethynyl)anthracene (**12**)*

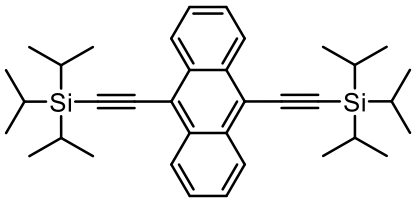

Method I. According to **general method A**, the Sonogashira coupling was carried out with (triisopropylsilyl)acetylene (**5**) as appropriate alkyne. The obtained product was purified by column chromatography (petroleum ether) as orange solid (**12**) (yield 79%). M.p. 212 – 213 °C.

Method II. According to **general method B**, the Sonogashira coupling was carried out with (triisopropylsilyl)acetylene (**5**) in microwave at 120 °C for 1 hours. Chromatographic purification was not performed due to a clean TLC – a single spot of target product. The obtained product (**12**) was recrystallized from toluene/methanol as yellow-orange solid (yield 92%). M.p. 212 – 213 °C. ^{1}H NMR (400 MHz, $CDCl_3$) δ 8.43 (dd, *J* = 6.7, 3.2 Hz, 4H), 7.40 (dd, *J* = 6.7, 3.3 Hz, 4H), 1.06 (d, *J* = 4.8 Hz, 42H). ^{13}C NMR (100 MHz, $CDCl_3$) δ 132.4, 127.3, 126.8, 118.7, 104.8, 103.3, 18.9, 11.5.

*(Bromoethynyl)triisopropylsilane (**6a**)*

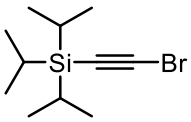

Adapted from a report procedure [32]. To a round bottom flask under argon was added (triisopropylsilyl)acetylene (**5**) (0.5 ml, 0.407 g, 2.23 mmol, 1 eq.), *N*-bromosuccinimide (0.476 g, 2.68 mmol, 1.2 eq.), $AgNO_3$ (0.359 g, 2.23 mmol, 1 eq.) in dry acetone. The reaction mixture was stirred at 20 °C for 2 h. Then solution was quenched with H_2O and extracted with petroleum ether. Combined organic layers were washed with brine and dried over Na_2SO_4. Solvent was removed under reduced pressure. The product was obtained as a colourless oil (**6a**) (0.57 g, 98%). ^{1}H NMR (400 MHz, $CDCl_3$) δ 0.86 (d, *J* = 1.5 Hz, 21H). ^{13}C NMR (100 MHz, $CDCl_3$) δ 83.5, 61.7, 18.5, 11.3.

*2-Methyl-6-(triisopropylsilyl)hexa-3,5-diyn-2-ol (**6b**)*

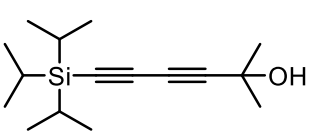

According to reported procedure [32] To a round bottom flask flushed with argon was added 2-methylbut-3-yn-2-ol (**6c**) (0.637 ml, 0.550 g, 6.54 mmol, 3 eq.), pyrrolidine (0.546 ml, 0.465 g, 6.54 mmol), CuCl (0.065 g, 0.65 mmol, 30mol%), $HONH_2$·HCl (0.152 g, 2.18 mmol, 1 eq.) in MeOH/H_2O (2:1). Mixture was cooled in ice bath and (bromoethynyl)triisopropylsilane (**6a**) (0.57 g, 2.18 mmol, as 0.45M MeOH solution, 1 eq.) was added slowly under argon. The reaction was then allowed to stir for 16 hours at 20 °C. After this time the reaction was quenched with H_2O and

diluted with Et_2O. The organic layer was then extracted with Et_2O and washed with aq. NH_4Cl and brine. The combined organic layers were then dried over $MgSO_4$. Solvent was removed under reduced pressure. The product was then obtained as a cream oil (**6b**) (0.525 g, 91%). ^1H NMR (400 MHz, $CDCl_3$) δ 1.47 (s, 6H), 1.01 (s, 21H).

*(Buta-1,3-diyn-1-yl)triisopropylsilane (**6**)*

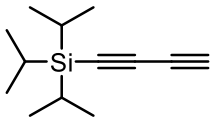

To compound (**6b**) (0.5 g, 1.89 mmol, 1 eq.) in anhydrous toluene under argon was added *tert*-BuOK (0.424 g, 3.78 mmol, 2 eq.). The mixture was stirred for 2 hours at 80 °C. Then solution was poured in H_2O, extracted with Et_2O. Combined organic layers were washed with brine and dried over $MgSO_4$. Solvent was removed under reduced pressure and obtained residue was purified by column chromatography (petroleum ether), giving pale orange oil (**6**) (0.371 g, 95%), that was used immediately.

*9,10-Bis((triisopropylsilyl)buta-1,3-diyn-1-yl)anthracene (**13**)*

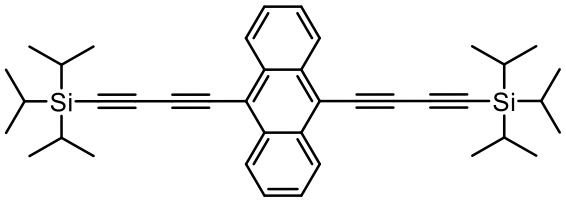

According to **general method A**, the Sonogashira coupling was carried out with (**6**) as appropriate alkyne. The obtained product was purified by column chromatography (petroleum ether) as bright yellow solid (**13**) (yield 81%). M.p. 213 – 215 °C. ^1H NMR (400 MHz, $CDCl_3$) δ 8.50 (dd, J = 6.7, 3.2 Hz, 4H), 7.56 (dd, J = 6.7, 3.2 Hz, 4H), 1.14 – 1.09 (m, 42H). ^{13}C NMR (100 MHz, $CDCl_3$) δ 133.5, 127.5, 127.2, 117.7, 92.6, 89.6, 87.6, 72.5, 18.7, 11.4.

*Prop-2-yne-1,1,1-triyltribenzene (**7**)*

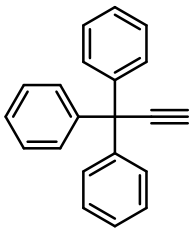

To solution of triphenylmethyl chloride (**7a**) (0.5 g, 1.79 mmol, 1 eq.) in anhydrous toluene under argon was added ethynylmagnesium bromide (0.5M in THF, 14 ml, 7.16 mmol, 4 eq.). Mixture was stirred under reflux for 16 hours. Then the solution was cooled, quenched with cold aq. NH_4Cl and extracted with CH_2Cl_2. Combined organic layers were washed with brine and dried over Na_2SO_4. Solvent was removed under reduced pressure and residue was purified by column

chromatography on silica using petroleum ether. Prop-2-yne-1,1,1-triyltribenzene (**7**) (0.406 g, 85%) was obtained as white solid and used immediately after purification.

*9,10-Bis(3,3,3-triphenylprop-1-yn-1-yl)anthracene (**14**)*

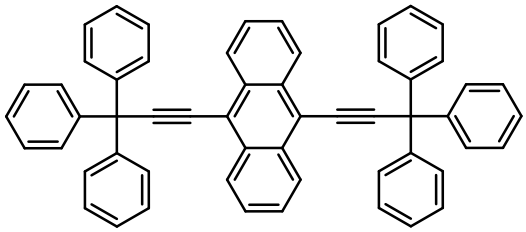

According to **general method A**, the Sonogashira coupling was carried out with (**7**) as appropriate alkyne. The obtained product was purified by column chromatography (petroleum ether/ethyl acetate 90:10) and recrystallized from toluene/methanol as a bright yellow solid (**14**) (yield 83%). M.p. 300 – 302 °C. ^{1}H NMR (400 MHz, $CDCl_3$) δ 8.57 (dd, *J* = 6.7, 3.2 Hz, 4H), 7.57 – 7.51 (m, 16H), 7.44 – 7.38 (m, 12H), 7.37 – 7.33 (m, 6H). ^{13}C NMR (100 MHz, $CDCl_3$) δ 145.3, 132.6, 129.4, 128.2, 127.3, 127.1, 126.7, 118.5, 108.4, 82.6, 57.2.

*Ethynyltriphenylsilane (**8**)*

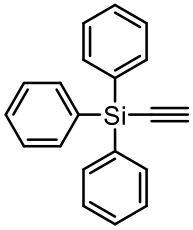

Compound (**8**) was synthesized from chlorotriphenylsilane (**8a**), and isolated according to the procedure described for the preparation of compound (**7**). Eluent for column chromatography – petroleum ether. Ethynyltriphenylsilane (**8**) (yield 90%) was obtained as white solid and used immediately after purification.

*9,10-Bis((triphenylsilyl)ethynyl)anthracene (**15**)*

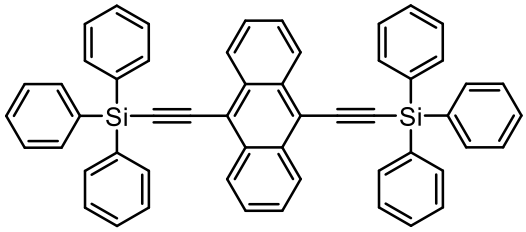

Method I. According to **general method A**, the Sonogashira coupling was carried out with (**8**) as appropriate alkyne. Eluent for column chromatography – petroleum ether/ethyl acetate (95:5). Recrystallized from toluene/methanol as yellow solid. Yield 52%. M.p. 253 – 254 °C.

Method II. According to **general method B**, the Sonogashira coupling was carried out with ethynyltriphenylsilane (**8**) in microwave at 120 °C for 1 hours. Eluent for column chromatography – petroleum ether/ethyl acetate (95:5). Recrystallized from toluene/methanol as yellow solid. Yield 87%. M.p. 253 – 254 °C.

Method III. Compound (**15**) was synthesized from (**16**) and (**8a**) and isolated according to the procedure described for the preparation of compound (**20**). Eluent for column chromatography – petroleum ether. Recrystallized from toluene/methanol as yellow solid. Yield 54%. M.p. 253 – 254 °C. ^{1}H NMR (400 MHz, $CDCl_3$) δ 8.70 (dd, *J* = 6.7, 3.3 Hz, 4H), 7.89 (d, *J* = 6.8 Hz, 12H), 7.63 (dd, *J* = 6.7, 3.3 Hz, 4H), 7.52 (dd, *J* = 9.1, 6.5 Hz, 18H). ^{13}C NMR (100 MHz, $CDCl_3$) δ 135.8, 133.5, 132.7, 130.3, 130.2 128.2, 127.3, 118.5, 105.96, 103.3.

CONCLUSIONS

1. Seven 9,10-diethynylanthracene derivatives (***10***–***15***, ***20***) were synthesized in moderate to excellent yields (52–92%). Microwave-assisted Sonogashira coupling reduced reaction times from 16–24 hours to 1–2 hours; compound ***12*** was isolated in 92% yield by recrystallization without chromatography.

2. Across the entire series, φ_{ISC} = 100% and $\varphi_{TET} \geq$ 98% were confirmed for all annihilators. All performance differences therefore originate from annihilator-side properties – φ_{FL}, φ_{TTA}, and f – rather than from sensitization efficiency.

3. The trityl-substituted compound ***14*** gave the highest φ_{UC} = 25.5% (f = 80.9%, φ_{TTA} = 95.5%), approaching DPA (φ_{UC} = 24.0%). Its sp^3-hybridized trityl carbon provides steric shielding without electronic conjugation with the anthracene π-system, preserving φ_{FL} = 66.5% and suppressing concentration quenching and photodimerization. The combination of these two factors is proposed as the structural basis for its outstanding TTA-UC performance.

4. Comparison of the silicon- and germanium-containing compounds (***12*** vs. ***20***) shows a decrease in φ_{FL} (56–71% vs. 55%) and φ_{UC} (14.8–20.6% vs. 12.2%) upon substitution of Si by Ge. This trend is consistent with stronger spin-orbit coupling at the heavier Ge center promoting non-radiative S_1 decay, although a definitive mechanistic assignment would require additional experiments and is beyond the scope of this work.

5. Extension of the alkyne spacer to a diyne unit (***13***) completely suppresses measurable upconversion, and doubly bridged anthracene derivatives show φ_{UC} < 5%. Both effects are consistent with a bathochromic shift in T_1 that reduces the driving force for energy transfer from PtOEP and diminishes the available anti-Stokes shift, though the relative contributions of these factors were not independently quantified.

6. Synthesis of tin-containing (***24***, ***25***) and adamantyl-substituted (***26***) targets was unsuccessful despite extensive optimization. For organotin derivatives, product instability toward protodestannylation is proposed as the most likely cause; for the adamantyl compound, the steric inaccessibility of the bridgehead carbon under all tested nucleophilic and electrophilic conditions precluded product formation. Both targets remain open challenges for future work.

SUMMARY

A series of seven 9,10-diethynylanthracene derivatives bearing triethylsilyl (***11***), triisopropylsilyl (***12***), triphenylsilyl (***15***), triphenylmethyl (***14***), triethylgermyl (***20***), TIPS-diynyl (***13***), and n-hexyl (***10***) substituents were synthesized in 52–92% yield by Sonogashira cross-coupling and lithium acetylide addition, and evaluated as annihilators for TTA-UC with PtOEP as sensitizer. Triplet sensitization was quantitative across the series (φ_{ISC} = 100%, $\varphi_{TET} \geq 98\%$), placing all performance differences in the annihilator domain. The trityl compound ***14*** gave φ_{UC} = 25.5% (f = 80.9%) – the highest in the series and on par with the benchmark DPA – attributed to the unique combination of steric protection and the absence of electronic conjugation at the sp^3-trityl center. A decrease in φ_{FL} and φ_{UC} observed for the Ge-containing compound ***20*** relative to its Si analogue ***12*** is consistent with stronger spin-orbit coupling at the heavier center promoting non-radiative decay, though this interpretation remains a hypothesis pending further investigation. Extension of the alkyne spacer or ring fusion of the anthracene core suppressed upconversion in both cases, consistent with T_1 energy mismatch with the PtOEP sensitizer. Microwave-assisted Sonogashira coupling reduced reaction times ten-fold and enabled chromatography-free isolation in several cases. Attempts to access tin-containing and adamantyl-substituted derivatives were unsuccessful – attributed tentatively to product protodestannylation and bridgehead inaccessibility, respectively – and remain targets for future work.

REFERENCES

[1] Parker, C.A., Hatchard, C.G., Delayed fluorescence from solutions of anthracene and phenanthrene, Proceedings of the Royal Society of London. Series A 269 (1962) 574–584. https://doi.org/10.1098/rspa.1962.0197.

[2] Singh-Rachford, T.N., Castellano, F.N., Photon upconversion based on sensitized triplet-triplet annihilation, Coordination Chemistry Reviews 254 (2010) 2560–2573. https://doi.org/10.1016/j.ccr.2010.01.003.

[3] Yanai, N., Kimizuka, N., Photon upconversion in molecular assemblies and framework materials, Chemical Society Reviews 45 (2016) 7344–7357. https://doi.org/10.1039/C6CS00412A.

[4] Fujimoto, K., Synthesis and photophysical properties of alkynylanthracene derivatives, Tetrahedron Letters 58 (2017) 4003–4006. https://doi.org/10.1016/j.tetlet.2017.09.015.

[5] Radiunas, E., Kazlauskas, K., NIR-to-blue photon upconversion in 9,10-bis((triisopropylsilyl)ethynyl)anthracene, Journal of Materials Chemistry C 8 (2020) 5525–5534. https://doi.org/10.1039/C9TC06031F.

[6] Radiunas, E., Naimovičius, L., Raišys, S., Jozeliūnaitė, A., Orentas, E., Kazlauskas, K., Efficient NIR-to-vis photon upconversion in binary rubrene films deposited by simplified thermal evaporation, Journal of Materials Chemistry C 10 (2022) 6314–6323. https://doi.org/10.1039/D1TC05332A.

[7] Naimovičius, L., Radiunas, E., Chatinovska, B., Jozeliūnaitė, A., Orentas, E., Kazlauskas, K., Functionalized diketopyrrolopyrrole compounds for NIR-to-visible photon upconversion, Journal of Materials Chemistry C 11 (2023) 698–704. https://doi.org/10.1039/D2TC03593F.

[8] Bharmoria, P., Bildirir, H., Moth-Poulsen, K., Triplet-triplet annihilation based near infrared to visible molecular photon upconversion, Chemical Society Reviews 49 (2020) 6529–6554. https://doi.org/10.1039/D0CS00257G.

[9] Naimovičius, L., Kazlauskas, K., The statistical probability factor in triplet mediated photon upconversion: a case study with perylene, Journal of Materials Chemistry C 11 (2023) 14826–14835. https://doi.org/10.1039/d3tc03158f.

[10] Lyons, A., Rigid molecular scaffolds for enhanced TTA upconversion, Angewandte Chemie International Edition 63 (2024) e202411003. https://doi.org/10.1002/anie.202411003.

[11] Gray, V., Dreos, A., Erhart, P., Albinsson, B., Moth-Poulsen, K., Abrahamsson, M., Photophysics and structure of 9,10-disubstituted anthracene

chromophores for triplet-triplet annihilation photon upconversion, Journal of Materials Chemistry C 3 (2015) 11111–11121. https://doi.org/10.1039/C5TC02431E.

[12] Anthony, J.E., Functionalized acenes and heteroacenes for organic electronics, Chemical Reviews 106 (2006) 5028–5048. https://doi.org/10.1021/cr050966z.

[13] Naimovičius, L., Dapkevičius, M., Radiunas, E., Miroshnichenko, M., Kreiza, G., Alcaide, C., Baronas, P., Sasaki, Y., Yanai, N., Kimizuka, N., Pun, A.B., Solà, M., Bharmoria, P., Kazlauskas, K., Moth-Poulsen, K., Enhancing the statistical probability factor in triplet-triplet annihilation photon upconversion via TIPS functionalization, Chemical Science 16 (2025) 20255–20264. https://doi.org/10.1039/D5SC05248C.

[14] Monguzzi, A., Tubino, R., Hoseinkhani, S., Campione, M., Meinardi, F., Low power, non-coherent sensitized photon up-conversion: modelling and perspectives, Physical Chemistry Chemical Physics 14 (2012) 4322–4332. https://doi.org/10.1039/c2cp23900k.

[15] Yanai, N., Kimizuka, N., Recent emergence of photon upconversion based on triplet energy migration in molecular assemblies, Chemical Communications 52 (2016) 5354–5370. https://doi.org/10.1039/C6CC00089D.

[16] Yanai, N., Kimizuka, N., Stimuli-responsive molecular photon upconversion, Angewandte Chemie International Edition 59 (2020) 10252–10264. https://doi.org/10.1002/anie.202001325.

[17] Duan, P., Maximizing singlet generation in triplet-triplet annihilation upconversion, Materials Chemistry Frontiers 7 (2023) 580–595. https://doi.org/10.1039/D3QM00069A.

[18] Bossanyi, D.G., Sasaki, Y., Wang, S., Chekulaev, D., Kimizuka, N., Yanai, N., Clark, J., Spin statistics for triplet-triplet annihilation upconversion: exchange coupling, intermolecular orientation, and reverse intersystem crossing, JACS Au 1 (2021) 2188–2201. https://doi.org/10.1021/jacsau.1c00322.

[19] Islangulov, R.R., Lott, J., Weder, C., Castellano, F.N., Noncoherent low-power upconversion in solid polymer films, Journal of the American Chemical Society 129 (2007) 12652–12653. https://doi.org/10.1021/ja075014k.

[20] Nishimura, N., Gray, V., Allardice, J.R., Zhang, Z., Pershin, A., Beljonne, D., Rao, A., Photon upconversion from near-infrared to blue light with TIPS-anthracene as annihilator, ACS Materials Letters 1 (2019) 660–664. https://doi.org/10.1021/acsmaterialslett.9b00287.

[21] Saltiel, J., Spin-statistical factors in diffusion-controlled reactions, Journal of the American Chemical Society 105 (1983) 7569–7578. https://doi.org/10.1021/ja00364a014.

[22] Berlman, I.B., Handbook of Fluorescence Spectra of Aromatic Molecules, Academic Press, 1971.

[23] Gray, V., Macromolecular annihilators and polymer-bound upconversion emitters, Chemistry - A European Journal 26 (2020) 11635–11645. https://doi.org/10.1002/chem.202001150.

[24] Bogdan, E., Synthesis and photophysics of dialkynylanthracene annihilators, Journal of Materials Chemistry C 8 (2020) 11687–11697. https://doi.org/10.1039/D0TC02315A.

[25] Schulze, T.F., Schmidt, T.W., Photochemical upconversion: present status and prospects for its application to solar energy conversion, Energy and Environmental Science 8 (2015) 103–125. https://doi.org/10.1039/C4EE02493C.

[26] Liang, L., Liu, X., Hu, Y., Chen, W., Guo, H., Liu, Y., Blue-emissive upconversion nanoparticles for low-power-excited bioimaging in vivo, Journal of the American Chemical Society 134 (2012) 4516–4519. https://doi.org/10.1021/ja3003638.

[27] Beck, L.R., Xie, K.A., Lainhart, B.C., Sherwood, T.C., Welin, E.R., Joe, C.L., Rovis, T., Dual nickel/photoredox-catalyzed aryl etherification enabled by an oxidative near-infrared-to-blue triplet-triplet annihilation upconversion system, ACS Catalysis 14 (2024) 18515–18522. https://doi.org/10.1021/acscatal.4c06084.

[28] Lissau, J.S., Singlet fission and triplet-triplet annihilation in rubrene derivatives, Nature Communications 13 (2022) 3105. https://doi.org/10.1038/s41467-022-31050-x.

[29] Narayanan, P., Nanoengineering triplet-triplet annihilation upconversion, ACS Nano 18 (2024) 2341–2355. https://doi.org/10.1021/acsnano.4c01453.

[30] Shockley, W., Queisser, H.J., Detailed balance limit of efficiency of p-n junction solar cells, Journal of Applied Physics 32 (1961) 510–519. https://doi.org/10.1063/1.1736034.

[31] Mori, H., Ono, Y., Nakagawa, S., Akima, S., Murakami, M., Korenaga, T., Nakaji-Hirabayashi, T., Kyogoku, M., Horino, Y., Synthesis of vinylidenecyclopropanes via gold(i)-catalyzed cyclopropanation of vinyl arenes with gamma-stannylated propargyl esters, Chemical Communications 60 (2024) 13518–13521. https://doi.org/10.1039/D4CC04384G.

[32] Wang, G., Synthetic methodology for alkynylation of condensed aromatics, Organic Letters 22 (2020) 4530–4534. https://doi.org/10.1021/acs.orglett.0c00733.

[33] Kondakov, D.Y., Triplet annihilation exceeding spin statistical limit in organic light-emitting diodes, Journal of Applied Physics 106 (2009) 124510. https://doi.org/10.1063/1.3273407.